UDK 621.791:661.862
Original scientific article/Izvirni znanstveni članek

ISSN 1580-2949
MTAEC9, 58(1)103(2024)

A NEW TYPE OF PLUG-IN FRICTION-STIR LAP WELDING BASED ON THE 6061-T6 ALUMINUM ALLOY

RAZISKAVA NOVE VRSTE VRTILNO-TRENJSKEGA VARJENJA ZLITINE NA OSNOVI ALUMINIJA VRSTE 6061-T6

Gaowei Cao, Jin Wang*, Bo Gao, Kaicheng Mu, Hui Zhang, Baoge Li

School of Mechanical and Automotive Engineering, Qingdao University of Technology, Qingdao 266520, China.

Prejem rokopisa – received: 2023-03-29; sprejem za objavo – accepted for publication: 2023-12-21

doi:10.17222/mit.2023.839

In this study a new type of plug-in friction-stir lap welding (PFSLW) is proposed to prepare welded joints based on 4-mm-thick 6061-T6 aluminum alloy sheet. The differences in the cross-sectional morphology, microstructure, cross-sectional hardness and shear properties between the PFSLW joint and the normal friction-stir lap-welding (FSLW) joint are discussed. The results show that the cross-sectional morphology of the PFSLW joint has undergone changes. The PFSLW joint has a mechanical interlocking structure on the advancing side that is beneficial to the connection strength of the joint. The grain structure differs at the boundary between the thermo-mechanically affected zone (TMAZ) and the heat-affected zone (HAZ), and the PFSLW joints show a more pronounced bending deformation of the grain organization near the boundary. The microhardness of PFSLW joints was increased in the TMAZ and HAZ areas, and the lowest hardness is further away from the center of the weld. The failure load of the PFSLW joint has been improved, the microcracks part of the PFSLW joint has a ridge-like structure. In addition, the actual welding width of PFSLW joints was improved.

Keywords: Plug-in friction-stir lap welding, mechanical interlocking, microhardness, failure load.

V članku avtorji opisujejo nov tip varjenja s pomočjo trenja, ki so ga poimenovali priključno torno vrtilno lepalno varjenje (PFSLW; angl.: plug-in friction stir lap welding). Pri tem se izraz lepanje tehniško pojmuje kot fino ploskovno brušenje trdih materialov. Za medsebojno varjenje (spajanje) s tem postopkom so pripravili vzorce iz 4 mm debele pločevine iz Al zlitine vrste 6061-T6. Nato so obravnavali oziroma primerjali razlike, med PFSLW zvari in zvari izdelanimi s konvencionalnim tornim vrtilno-lepalnim varjenjem (FSLW), v morfologiji presekov zvarnih spojev, med mikrostrukturami, med trdotami vzdolž prečnih presekov in mehanskimi lastnostmi pod strižnimi obremenitvami. Rezultati preimerjave so pokazali pomembne spremembe morfologije preseka pri PFSLW zvarih. Ti zvari imajo mehansko spojeno strukturo na strani, ki je pomembna za trdnost zvarnega spoja. Kristalna struktura se razlikuje na meji med term-mehansko vplivano cono (TMAZ; angl.: thermo-mechanically affected zone) in toplotno vplivano cono (HAZ; angl.: heat-affected zone). PFSLW zvarni spoji imajo bolj izrazito deformacijo zaradi upogibne obremenitve blizu meje. Mikrotrdote PFSLW zvarnih spojev so bile očitno višje v TMAZ in HAZ in nižje v področjih daleč stran od sredine zvarnih spojev. Obremenitev pri porušitvi PFSLW je bila precej višja oz. izboljšana v primerjavi z FSLW in nastale mikrorazpoke so imele togo strukturo. Poleg tega so bile dejanske širine zvarnih spojev PFSLW močno (opazno) izboljšane.

Ključne besede: priključno vrtilno torno-lepalno varjenje, mehansko spajanje, mikrotrdota, obremenitev pri porušitvi

1 INTRODUCTION

Friction-stir welding (FSW) is a patented technology proposed by The Welding Institute (TWI) in the 1990s.[1] It was first applied to the welding of aluminum alloys with low melting points, and then gradually expanded to the welding of the same or dissimilar materials.[2] FSW is a solid-state joining technology, which can avoid defects such as porosity and cracks produced by the traditional fusion-welding process. It has been applied in structural manufacturing in aerospace, automobiles, shipbuilding and other fields, and has shown good prospects for engineering applications.[3,4] FSW has a variety of joint forms such as butt, lap, angle joint, and T-joint.[1,5,6] The high-performance butt joints that can be achieved by friction-stir welding have been confirmed in many studies.[7] Friction-stir lap welding (FSLW) joints are also an important form of joints, and lap joints are widely used in the assembly of various parts and products in the aerospace and automotive industries to replace riveted lap joints.[8] FSLW is extensively utilized in the fabrication of structural components for aircraft, including wings, tail sections, and fuselage segments. In the electric-vehicle sector, FSLW is employed in the manufacturing of battery casings, ensuring the structural integrity and safety of the battery compartment.

There has been a lot of research work on FSLW and many researchers have conducted a lot of research in order to improve the performance of lap joints. Ge et al.[9] studied the effects of pin length and welding speed on the quality of FSLW joints of dissimilar aluminum alloys. The research results show that optimizing the combination of pin length and welding speed can effectively improve the tensile strength of the joint. Sharma et al.[10] studied the addition an interlayer of graphene nanoplatelets (GNPs) at the lap interface of 6061 aluminum alloy. The results showed that the addition of the GNP interlayer increased the weld strength and percent-

*Corresponding author's e-mail:
jinwangqut@163.com (Jin Wang)

age elongation by 121 % and 53 %, respectively, compared to the weld without the GNP interlayer. Paranthaman et al.[11] used a modified-interlocking friction-stir-welding lap joint to join AA8011-AA7475 with different *w*/% of SiC particles. The results showed that the joints made with SiC particles exhibited better static properties and the hardness, tensile strength and elongation of AA8011-AA7475 joints were increased when the SiC content was 2 *w*/%. Kesharwani et al.[12] established a method for optimizing the groove width of AA6061-T6 plates filled with Al2O3 powder particles. They found that the tensile and yield strengths of specimens increased by 7 % and 20 %, respectively, for a groove width of 1 mm. Abegunde et al.[13] machined V-grooves in aluminum plates to fill titanium carbide particles and studied the effects of process parameters on the microstructure, microhardness and tensile properties under this condition.

In previous studies, many experimenters have tried to improve the strength of lap joints by changing the process parameters or adding interlayers at the lap interface. Some researchers have also grooved the surface of the sheet before welding, but the main purpose was to place particles or interlayers in the groove, and the research focus did not pay attention to the effect of the groove itself on the joint. In this study, a plug-in friction-stir lap welding (PFSLW) in which a groove is made at the lap interface and the two plates are plugged together is proposed. In this lap-joint mode, the contact area of the interface between the upper and lower plates is increased and there is mechanical occlusion before welding, and it also has the characteristics of a butt connection on the side of the groove. In this paper, the cross-sectional morphology, microstructure, microhardness and shear properties of the PFSLW are investigated. The research results are also of significance for related research that requires grooving to add intermediate materials.

2 EXPERIMENTAL PART

The schematic diagram of the plate is shown in **Figure 1a**. 6061-T6 aluminum alloy plate is used as the base material, and the plate size is 120 mm × 60 mm × 4 mm. A 2-mm width and 2-mm depth groove are cut in the plate, and a 13-mm-width and 2-mm-depth side groove are cut along the edge to complete the plug-in. The lap width of the two plates is 30 mm, and the welding line along the straight line in the middle of the two grooves is also the center line of the lap overlap area, as shown in **Figure 1b**. **Figure 1c** shows the stirring tool used, the pin is left-threaded and made of H13 steel, the pin length is 4.7mm. During the experiment, the stirring tool tilt angle of 2.5°, rotation speed of 1200 min^{-1}, welding speed of 120 mm/min, and the shoulder is inserted to a depth of 0.2 mm.

After the welding was completed, the lap shear specimens and metallographic specimens were cut out using an electrical discharge cutting machine, and the flash generated during the welding process was removed before cutting. The metallographic sample was polished with sandpaper, and etched with Keller reagent after polishing, and the metallographic organization and welding defects were observed with an optical microscope. Joint cross-section microhardness measurements were performed under a load of 100g and a dwell time of 10 s. The lap shear specimen standard is ASTM D3164, **Fig-**

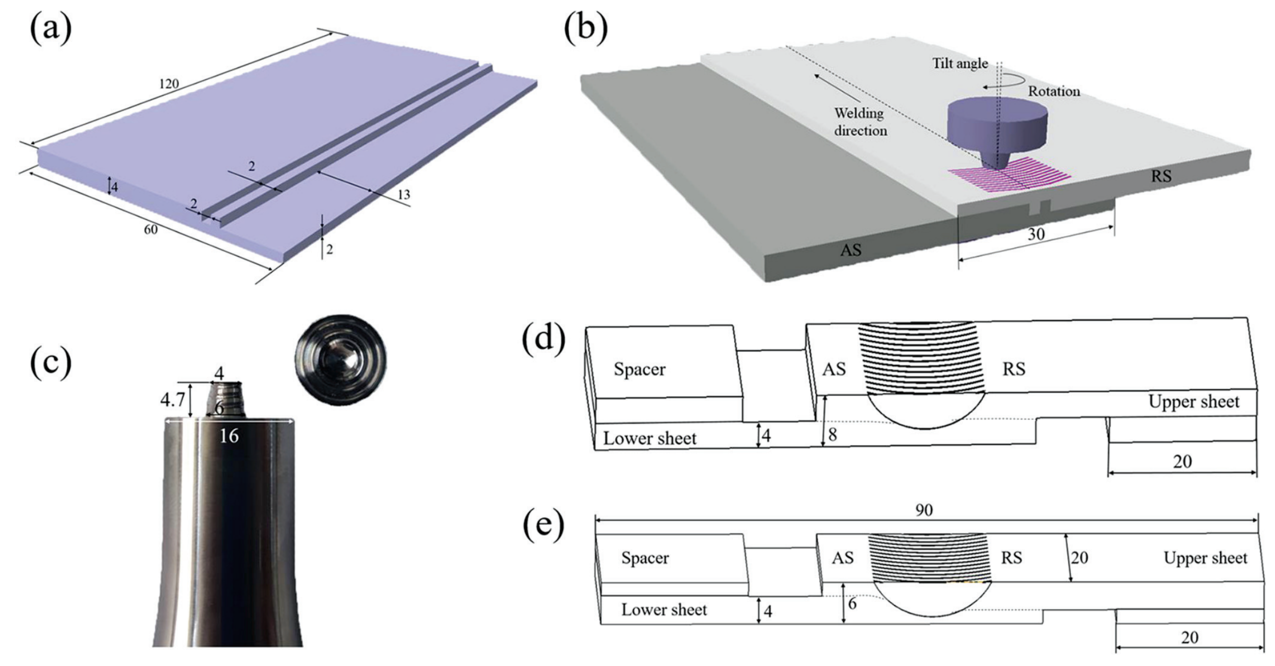

Figure 1: Dimensions of FSLW equipment and lap shear specimens: a) Base material, b) Schematic of PFSLW process, c) Friction stir welding tool, d) FSLW lap shear specimen, e) PFSLW lap shear specimen

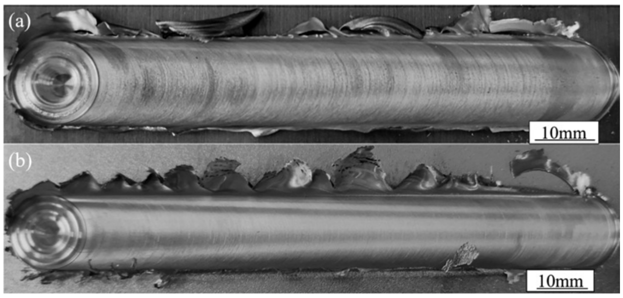

Figure 2: Joint surface morphology: a) FSLW, b) PFSLW

ure 1d and **1e** shows the FSLW lap shear specimens and PFSLW lap shear specimens with a width of 20 mm and a length of 90 mm, lap width of 30 mm, the two specimens differ only in the thickness of the lap area, but the rest of the parameters are identical, the specimens are cut along the vertical direction of the weld. Two shims are used at both ends of the specimen to make the thickness of both ends of the specimen consistent with the thickness of the lap area. The lap shear experiments were performed on an electronic universal tensile testing machine with a constant speed of 1 mm/min during the test, and the average value of three specimens was taken as the result for discussion. The fracture forms were observed and the fracture morphology was analyzed using a scanning electron microscope (SEM).

3 RESULTS AND DISCUSSION

3.1 Surface and cross-sectional morphology

During the FSW process, the high-speed rotating pin and shoulder drive the plasticized material on the AS to flow in the direction of the RS, and some of the material is extruded out of the joint due to the squeezing effect of the shoulder to form flash.[14] **Figure 2** shows the typical surface morphology of the FSLW and PFSLW under the same welding parameters, and both modes successfully prepared lap joints with good surfaces. In comparison, the surface morphology of the joint obtained under PFSLW conditions is smoother, and the shaft shoulder marks are not obvious. This is due to the presence of unavoidable gaps in the plug-in mode, and the material fills into the gaps during the plastic-flow process, resulting in less overflowing material.

Figure 3a and **Figure 4a** show the macroscopic images of the FSLW joint and the PFSLW joint cross-sections, and it can be seen that the joint has a bowl shape due to the joint action of the shoulder and the pin, and four typical zones can be observed in both cross-sections: the SZ, the thermo-mechanically affected zone (TMAZ), the heat-affected zone (HAZ) and the BM.[9] HD and CLD are typical features of lap joints,[1] which are caused by the penetration of the tool through the lower plate at a certain depth, the original plate interface on both sides of the weld is slightly bent upward or downward depending on the tool geometry and the welding parameters,[15] the defects appearing on the AS side are called HD and the defects on the RS side are called CLD. It has been shown that the extension direction of the hook defect can be either upward or downward.[16]

Figure 3b and **Figure 4b** show the AS side hook structure of the FSLW and PFSLW. A complex and tortuous interface geometry appears in the PSFLW hook structure, as shown in **Figure 4b** and **Figure 5a**, where the upper and lower plates are inserted and occluded

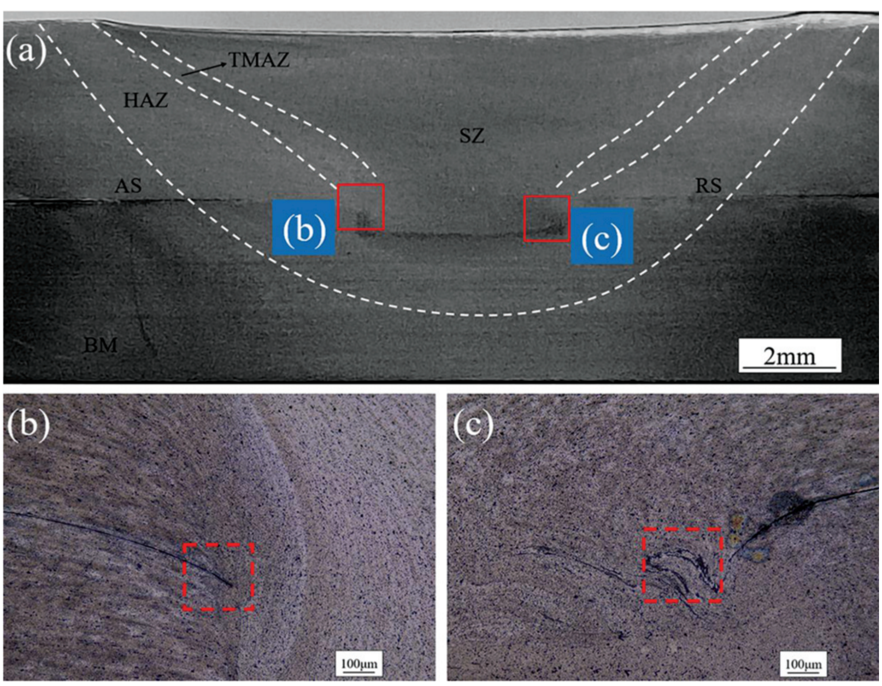

Figure 3: Cross-sections of the FSLW joints: a) Cross-sectional macroscopic morphology, b) HD, c) CLD

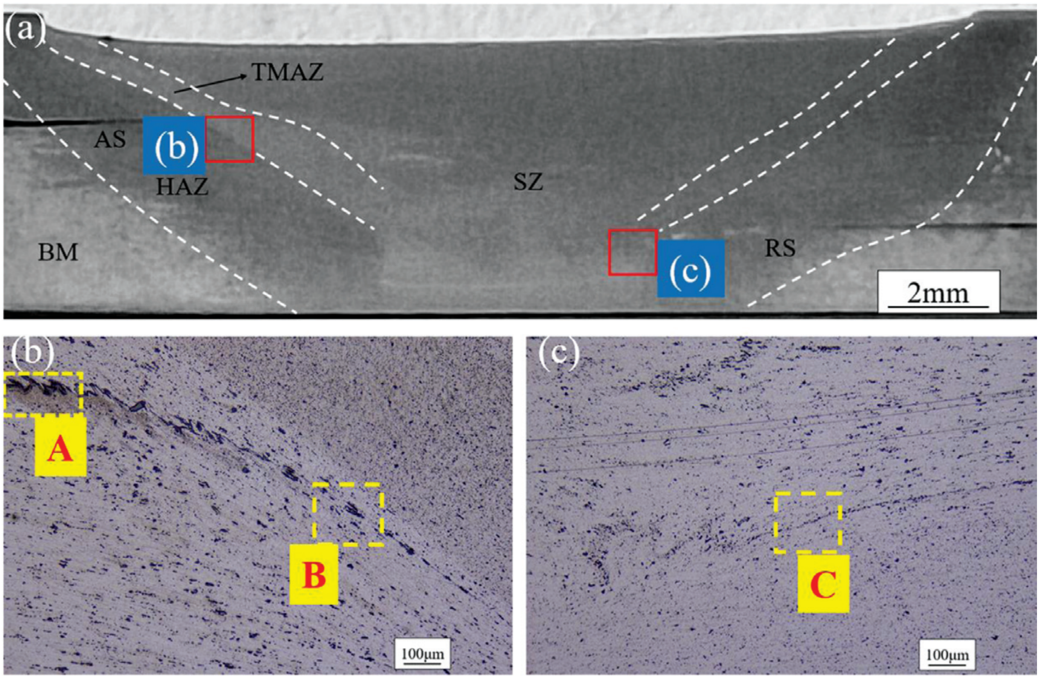

Figure 4: Cross-sections of the PFSLW joints: a) Cross-sectional macroscopic morphology, b) HD, c) CLD

with each other, forming a mechanical interlocking structure, which is not found in the normal FSLW. It has been shown that similar such interlocking structure increases the effective contact area between the upper and lower plates, which is beneficial for improving the weld joint's strength,[17] so the appearance of such mechanical interlocking structure may be able to be a useful structure to improve the joint strength of lap joints. At the same time, microcracks appear at the end of the joint interface, forming part of the hook structure in PFSLW, which is also not present in the AS side hook structure of normal FSLW joints. **Figure 3c** and **Figure 4c** show the RS side cold lap structures of FSLW and PFSLW.

Figure 5b and **5c** show the SEM images of microcracks on the AS side and RS side of the PFSLW, where it can be observed that some of the microcracks are fully connected, indicating that although the microcracks are defect extensions and are likely to become crack extensions during fracture, they can improve the joint strength of the joint to a certain extent compared to the defects without connected parts.

3.2 Microstructure

Figure 6 and **Figure 7** show the microstructure of different areas of the FSLW and PFSLW joints. Elongated slate-like organization and equiaxed grains can be observed in the TMAZ region, with a clearer boundary between the HAZ and TMAZ on the AS side (**Figure 6b** and **Figure 7b**), while in the RS-side TMAZ (**Figure 6d** and **Figure 7d**), the tissue evolution is more complicated due to the complex flow of extruded metal, and no obvious boundary occurs.[18] The TMAZ was subjected to less mechanical stirring, which caused only a large bending deformation in this part of the tissue, while partial recrystallization occurred by a local reversion reaction due to the thermal cycling.[19] In TMAZ at the same distance position from the upper plate surface, the down-

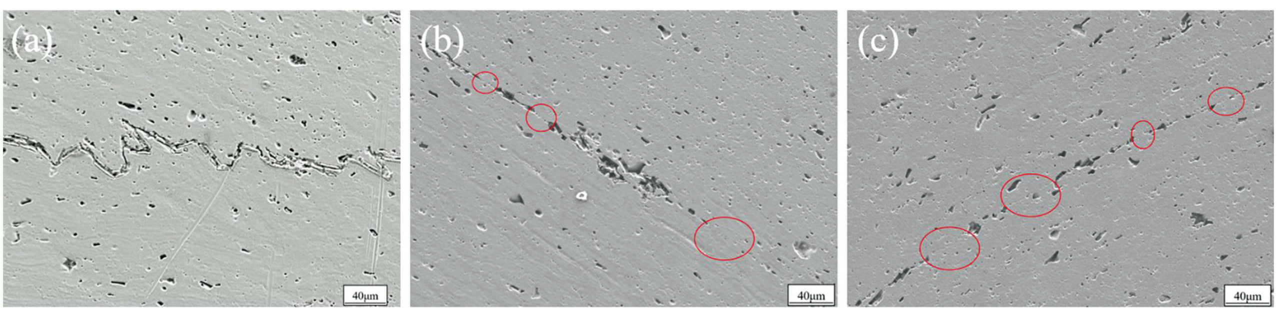

Figure 5: A(a), B(b), C(c) in **Figure 4:** a) Mechanical interlocking structure, b) SEM image of microcracks on the AS side, c) SEM image of microcracks on the RS side

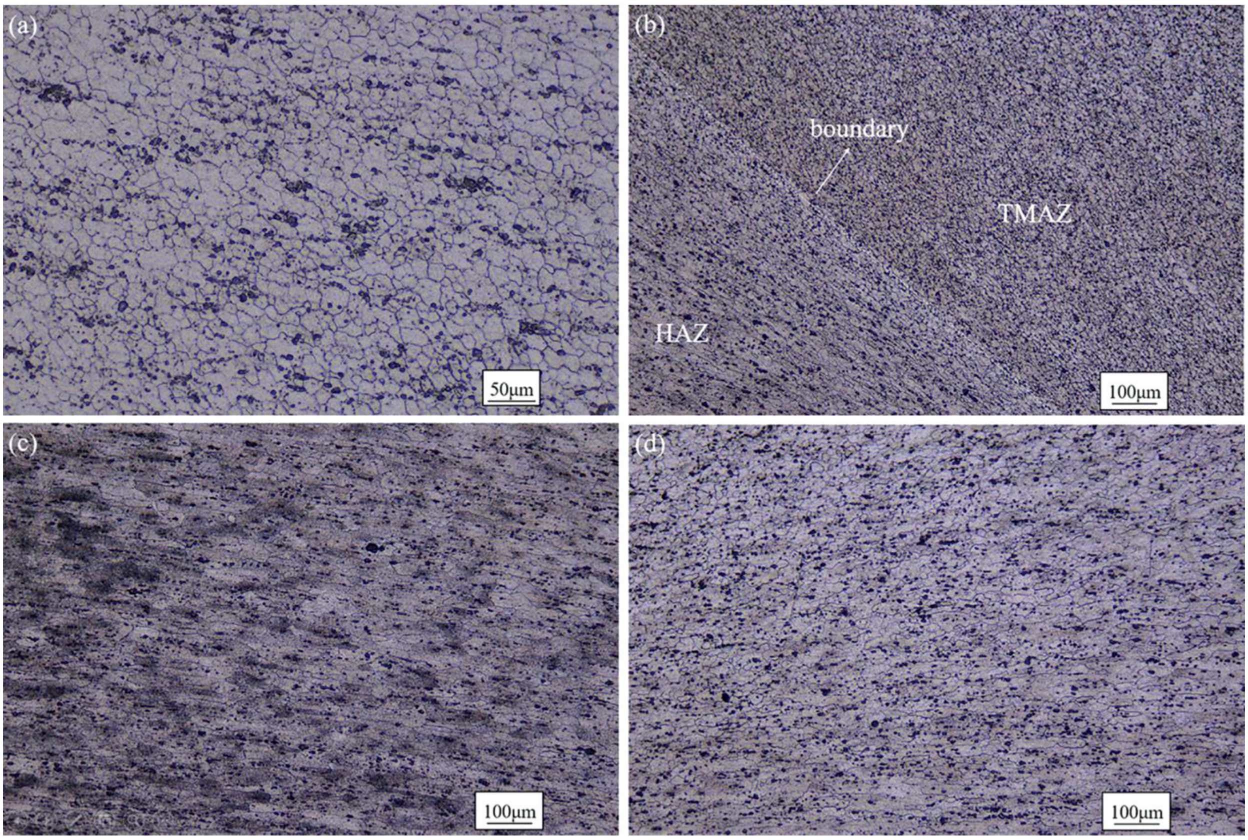

Figure 6: FSLW joint microstructure: a) SZ, b) TMAZ on AS, c) HAZ, d) TMAZ on RS

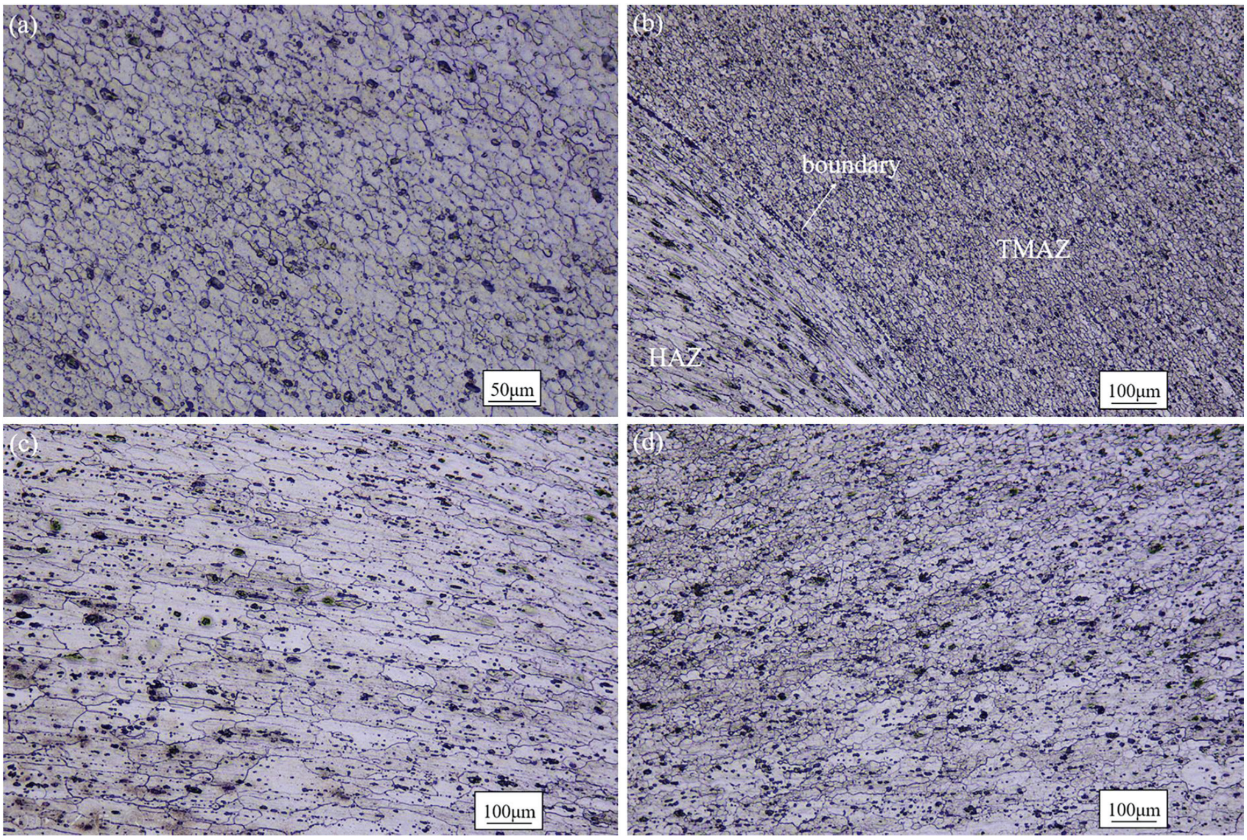

Figure 7: PFSLW joint microstructure: a) SZ, b) TMAZ on AS, c) HAZ, d) TMAZ on RS

ward elongated slat-like tissue around the boundary line in PFSLW has more obvious bending deformation, which can be explained by the presence of the downward-bending hook structure here, which is subjected to less deformation resistance when affected by thermal machine action.

SZ was simultaneously subjected to strong mechanical stirring and thermal cycling at higher temperatures, and the strong plastic deformation and high temperature led to dynamic recrystallization of the original slate-like organization of the BM and the formation of refined equiaxed grains (**Figure 6a** and **Figure 7a**).[20] HAZ tissue was only subjected to weaker thermal cycling during the welding process, and no significant deformation occurred, forming a rough slate-like organization similar to that of the BM (**Figure 6c** and **Figure 7c**).

3.3 Microhardness

The results of the FSLW and PFSLW microhardness tests are shown in **Figure 8**, and the hardness-test locations are both located at 3 mm from the upper plate. The hardness distribution of both models showed a typical W-shaped feature, which is similar to the distribution results of the previous study content.[21] Microhardness values in the weld area as well as in the weld-affected area with varying degrees of decrease compared to the base material. SZ area due to the strong mechanical stirring and high temperature makes the dissolution of the precipitation phase during the welding process, reducing the hardness of the SZ area, but the hardness values here are higher than HAZ and TMAZ because of the dynamic recrystallization that occurs here to generate finer grains.[18] The material is subjected to weaker thermal and mechanical effects in the TMAZ region, where the grains undergo bending deformation and partial recrystallization causing an increase in dislocation density, and an increase in hardness in the TMAZ toward the center of the weld.[22] In the HAZ region, the material undergoes thermal cycling, which changes the organization and mechanical properties, resulting in the lowest hardness values all occurring here.[23]

In the TMAZ and HAZ regions, the hardness values of the PFSLW joints are higher than the hardness values of the same region in the FSLW joints, which is particularly significant in the TMAZ region. In the HAZ region, where the hardness values are relatively low, the location of the lowest hardness values on the AS side and RS side of the PFSLW joint occur further from the center of the weld than in the FSLW joint. It is understood from the available studies that the roughness and contact area of the lap interface can have a significant effect on the heat-transfer efficiency.[24] In the PFSLW process, the presence of the plug-in slot increases the interface contact area between the upper and lower plates, which will enhance the heat-transfer efficiency between the upper and lower plates compared to the normal FSLW, and the enhanced thermal circulation can lead to faster dissolution of the precipitated phase in the SZ, resulting in a slight decrease in the hardness value in the SZ region. The presence of the plug-in slot also allows the heat-transfer efficiency to be enhanced in the lateral direction, and the thermomechanical effect produces a wider range of influence in the lateral direction, so that the hardness values in both the TMAZ and HAZ regions of the PFSLW joint are increased to a certain extent, and the location of the lowest hardness value generation is shifted laterally to the outside accordingly.

3.4 Shear performance

The load-displacement curves of the FSLW joint and PFSLW joint during the experiments are shown in **Figure 9**. The failure load of the PFSLW joint is generally larger than that of the FSLW joint. The average failure load of the FSLW joint is 7.434KN and the maximum

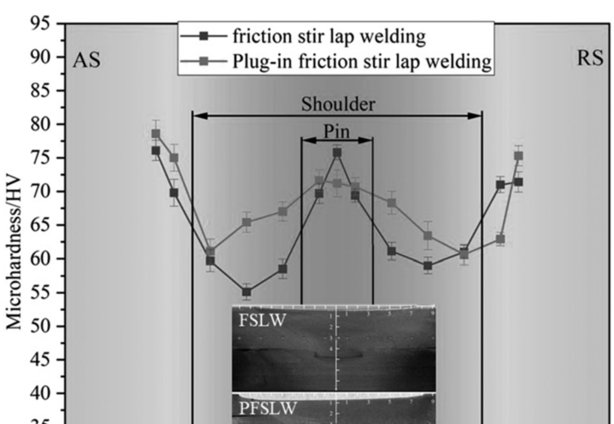

Figure 8: Microhardness curves and location chart

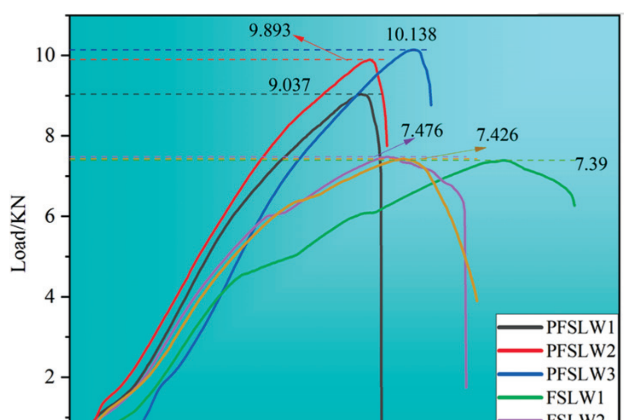

Figure 9: Load-displacement curves

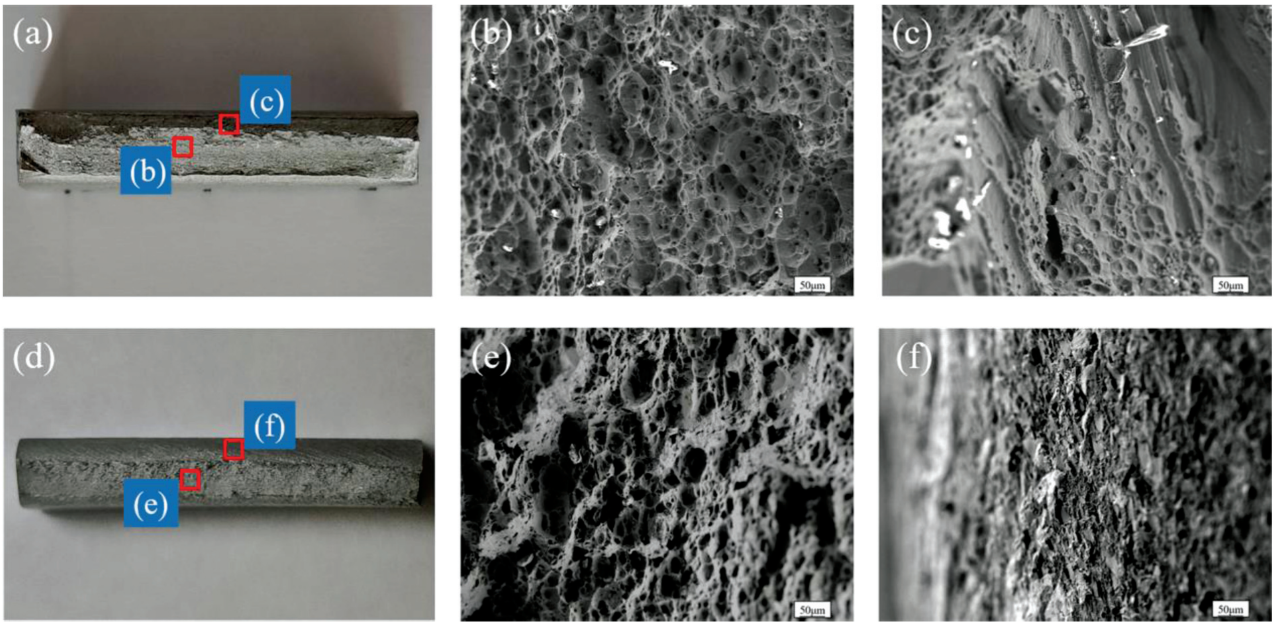

Figure 10: Fracture morphology diagram: a) FSLW, b) SEM diagram of FSLW joint, c) SEM image of HD side of FSLW fracture, d) PFSLW, e) SEM diagram of PFSLW joint, f) SEM image of microcrack side of PFSLW fracture

failure load is 7.476 kN, while the average failure load of the PFSLW joint is 9.67 kN and the maximum failure load reaches 10.138 kN, and the failure load of the PFSLW joint gets a 30 % increase.

Figure 10a and **10d** show the macroscopic morphology of the fractures of the FSLW specimen and the PFSLW specimen. To further clarify the fracture characteristics of the FSLW and PFSLW joints, the fracture morphology of the AS side of both joints is given in **Figure 10**. Many dimples can be observed in the diagram, indicating that both joints fracture in a ductile fracture mode[25]. The size of the dimples in **Figure 10b** is relatively uniform, while the presence of larger size dimples can be found in **Figure 10e**, indicating that the ductile fracture morphology is enhanced in the PFSLW joint fracture,[1] and this occurs probably because of the different thermal influences on the reinforcement of the joint. **Figure 10c** shows the fracture morphology of the HD side of the FSLW joint, where some of the smaller dimples and tear-like structures can be observed, indicating that there is a potential crack-propagation area here, which belongs to the weakening area of the connection strength. **Figure 10f** shows the fracture characteristics of the microcracks (**Figure 5b**) on the AS side of the PFSLW joint, it can be observed here that there is a layer of ridges without typical fracture characteristics, no effective metallurgical bond is formed here, and the bonding force is generated on this side mainly by the mechanical interlocking structure observed in **Figure 5a**.

4 CONCLUSIONS

The following conclusions can be drawn from this work:

- PFSLW mode joints have better joint surface quality and produce a complex mechanical interlocking structure appears on the AS side of the PFSLW joint, and the presence of this mechanical interlocking structure is beneficial for improving the joint strength.
- PFSLW joints have significantly higher microhardness in the TMAZ and HAZ regions than normal FSLW joints, PFSLW specimens have a wider effective welding width, the lowest hardness values occur farther from the weld centerline of PFSLW joints.
- The maximum failure load of PFSLW joints is 30% higher than that of FSLW joints, no effective metallurgical bond formed on the microcracked side of the PFSLW fracture, the mechanical interlocking structure plays the main connecting role here.

Acknowledgment

This work was supported by Key R&D projects of Shandong Province (Grant numbers 2019GGX102023).

5 REFERENCES

[1] Z. L. Zhou, Y. M. Yue, S. D. Ji, Z. W. Li, L. G. Zhang, Effect of rotating speed on joint morphology and lap shear properties of stationary shoulder friction stir lap welded 6061-T6 aluminum alloy, Int. J. Adv. Manuf. Technol., 88 (**2017**) 2135–2141, doi:10.1007/s00170-016-8924-6

[2] T. Singh, S. K. Tiwari, D. K. Shukla, Mechanical and microstructural characterization of friction stir welded AA6061-T6 joints reinforced with nano-sized particles, Mater. Char., 159 (**2020**) 110047, doi:10.1016/j.matchar.2019.110047

[3] S. Hassanifard, H. Alipour, A. Ghiasvand, A. Varvani-Farahani, Fatigue response of friction stir welded joints of Al 6061 in the absence

and presence of inserted copper foils in the butt weld, J. Manuf. Process., 64 (**2021**) 1–9, doi:10.1016/j.jmapro.2021.01.010

4 N. Nayan, M. Yadava, R. Sarkar, S. V. S. Narayana Murty, N. P. Gurao, S. Mahesh, M. J. N. V. Prasad, I. Samajdar, Microstructure and tensile response of friction stir welded Al–Cu–Li (AA2198-T8) alloy, Mater. Char., 159 (**2020**) 110002, doi:10.1016/j.matchar.2019.110002

5 S. B. Zeng, G. Q. Chen, I. Dinaharan, Q. Liu, S. Zhang, P. K. Sahu, J. J. Wu, G. Zhang, Q. Y. Shi, Microstructure and Tensile Strength of AA6082 T-joints by Corner Stationary Shoulder Friction Stir Welding: Effect of Tool Rotation Speed, J. Mater. Eng. Perform., 29 (**2020**) 7094–7103, doi:10.1007/s11665-020-05179-w

6 H. A. Derazkola, N. Kordani, H. A. Derazkola, Effects of friction stir welding tool tilt angle on properties of Al-Mg-Si alloy T-joint, CIRP-JMST., 33 (**2021**) 264–276, doi:10.1016/j.cirpj.2021.03.015

7 A. Kalinenko, I. Vysotskii, S. Malopheyev, S. Mironov, R. Kaibyshev, Relationship between welding conditions, abnormal grain growth and mechanical performance in friction-stir welded 6061-T6 aluminum alloy, Mater. Sci. Eng., A, 817 (**2021**) 141409, doi:10.1016/j.msea.2021.141409

8 V. Mertinger, B. Varbai, Y. Adonyi, J. DeBacker, E. Nagy, M. Leskó, V. Kárpáti, Microstructure evaluation of dissimilar AA2024 and AA7050 aluminum joints made by corner stationary-shoulder friction stir welding, Weld. World., 66 (**2022**) 1623–1635, doi:10.1007/s40194-022-01321-5

9 Z. H. Ge, S. S. Gao, S. D. Ji, D. J. Yan, Effect of pin length and welding speed on lap joint quality of friction stir welded dissimilar aluminum alloys, Int. J. Adv. Manuf. Technol., 98 (**2018**) 1461–1469, doi:10.1007/s00170-018-2329-7

10 A. Sharma, V. M. Sharma, A. Gugaliya, P. Rai, S. K. Pal, J. Paul, Friction stir lap welding of AA6061 aluminium alloy with a graphene interlayer, Mater. Manuf. Process., 35 (**2020**) 1532-2475, doi:10.1080/10426914.2020.1718694

11 V. Paranthaman, K. S. Sundaram, L. Natrayan, Influence of SiC Particles on Mechanical and Microstructural Properties of Modified Interlock Friction Stir Weld Lap Joint for Automotive Grade Aluminium Alloy, Silicon, 14 (**2022**) 1617–1627, doi:10.1007/s12633-021-00944-5

12 R. Kesharwani, K. K. Jha, M. Imam, C. Sarkar, The Optimization of Gap Width Size During Friction Stir Welding of AA 6061-T6 with Al2O3 Particle Reinforcement, J. Mater. Eng. Perform., (**2022**), doi:10.1007/s11665-022-07525-6

13 N. Dialami, M. Cervera, M. Chiumenti, Effect of the Tool Tilt Angle on the Heat Generation and the Material Flow in Friction Stir Welding, Metal., 9 (**2018**) 28, doi:10.3390/met9010028

14 O. O. Abegunde, E. T. Akinlabi, D. Madyira, Microstructure evolution and mechanical characterizations of Al-TiC matrix composites produced via friction stir welding, Mater. Tehnol., 51 (**2017**) 2, 297–306, doi:10.17222/mit.2016.033

15 F. Fadaeifard, K. A. Matori, M. Toozandehjani, A. R. Daud, M. K. A. M. Ariffin, N. K. Othman, F. Gharavi, A. H. Ramzani, F. Ostovan, Influence of rotational speed on mechanical properties of friction stir lap welded 6061-T6 Al alloy, Trans. Nonferrous Met. Soc. China, 24 (**2014**) 4, 1004-1011, doi:10.1016/S1003-6326(14)63155-1

16 R. J. Wang, H. T. Kang, X. H. Lei, Fatigue Performance and Strength Assessment of AA2024 Alloy Friction Stir Lap Welds, J. Mater. Eng. Perform., 29 (**2020**) 6701–6713, doi:10.1007/s11665-020-05145-6

17 Y. X. Huang, X. C. Meng, L. Zhou, Fundamental and Application of Friction Stir Welding, Harbin Institute of Technology Press, Harbin 2021, 242

18 E. Salari, M. Jahazi, A. Khodabandeh, H.G. Nanesa, Friction stir lap welding of 5456 aluminum alloy with different sheet thickness: process optimization and microstructure evolution, Int. J. Adv. Manuf. Technol., 82 (**2016**) 39–48, doi:10.1007/s00170-015-7342-5

19 C. Rajendran, K. Srinivasan, V. Balasubramanian, H. Balaji, P. Selvaraj, Effect of tool tilt angle on strength and microstructural characteristics of friction stir welded lap joints of AA2014-T6 aluminum alloy, Trans. Nonferrous Met. Soc. China, 29 (**2019**) 1824–1835, doi:10.1016/S1003-6326(19)65090-9

20 M. Yang, R. J. Bao, X. Z. Liu, C. Q. Song, Thermo-mechanical interaction between aluminum alloy and tools with different profiles during friction stir welding, Trans. Nonferrous Met. Soc. China, 29 (2**0**19) 495–506, doi:10.1016/S1003-6326(19)64958-7

21 W. Wang, S. N. Yuan, K. Qiao, K. S. Wang, S. Y. Zhang, P. Peng, T. Zhang, H. Peng, B. Wu, J. Yang, Microstructure and nanomechanical behavior of friction stir welded joint of 7055 aluminum alloy, J. Manuf. Process., 61 (**2021**) 311–321, doi:10.1016/j.jmapro.2020.11.016

22 H. J. Liu, Y. Q. Zhao, Y. Y. Hu, S. X. Chen, Z. Lin, Microstructural characteristics and mechanical properties of friction stir lap welding joint of Alclad 7B04-T74 aluminum alloy, Int. J. Adv. Manuf. Technol., 78 (**2015**) 1415–1425, doi:10.1007/s00170-014-6718-2

23 F. J. Liu, L. Fu, H. Y. Chen, Microstructure Evolution and Mechanical Properties of High-Speed Friction Stir Welded Aluminum Alloy Thin Plate Joints, J. Mater. Eng. Perform., 27 (**2018**) 3590–3599, doi:10.1007/s11665-018-3441-4

24 Y. X. Zhang, Y. X. Huang, X. C. Meng, J. C. Li, Y. M. Xie, Q. Fan, Friction stir lap welding of AA2024-T4 with drastically different thickness, Int. J. Adv. Manuf. Technol., 106 (**2020**) 3683–3691, doi:10.1007/s00170-019-04865-x

25 S. R. Govindaraj, S. Karuppan, Mechanical and metallurgical properties of friction-stir-welded AISI 304 stainless steel, Mater. Tehnol., 57 (**2023**) 2, 127–134, doi:/10.17222/mit.2022.678